

Video Article

Live Imaging of Drug Responses in the Tumor Microenvironment in Mouse Models of Breast Cancer

Elizabeth S. Nakasone^{1,2}, Hanne A. Askautrud^{2,3}, Mikala Egeblad²¹Watson School of Biological Sciences²Cold Spring Harbor Laboratory³Departments of Medical Genetics, University of Oslo and Oslo University HospitalCorrespondence to: Mikala Egeblad at egeblad@cshl.eduURL: <https://www.jove.com/video/50088>DOI: [doi:10.3791/50088](https://doi.org/10.3791/50088)

Keywords: Cancer Biology, Issue 73, Medicine, Molecular Biology, Cellular Biology, Biomedical Engineering, Genetics, Oncology, Pharmacology, Surgery, Tumor Microenvironment, Intravital imaging, chemotherapy, Breast cancer, time-lapse, mouse models, cancer cell death, stromal cell migration, cancer, imaging, transgenic, animal model

Date Published: 3/24/2013

Citation: Nakasone, E.S., Askautrud, H.A., Egeblad, M. Live Imaging of Drug Responses in the Tumor Microenvironment in Mouse Models of Breast Cancer. *J. Vis. Exp.* (73), e50088, doi:10.3791/50088 (2013).

Abstract

The tumor microenvironment plays a pivotal role in tumor initiation, progression, metastasis, and the response to anti-cancer therapies. Three-dimensional co-culture systems are frequently used to explicate tumor-stroma interactions, including their role in drug responses. However, many of the interactions that occur *in vivo* in the intact microenvironment cannot be completely replicated in these *in vitro* settings. Thus, direct visualization of these processes in real-time has become an important tool in understanding tumor responses to therapies and identifying the interactions between cancer cells and the stroma that can influence these responses. Here we provide a method for using spinning disk confocal microscopy of live, anesthetized mice to directly observe drug distribution, cancer cell responses and changes in tumor-stroma interactions following administration of systemic therapy in breast cancer models. We describe procedures for labeling different tumor components, treatment of animals for observing therapeutic responses, and the surgical procedure for exposing tumor tissues for imaging up to 40 hours. The results obtained from this protocol are time-lapse movies, in which such processes as drug infiltration, cancer cell death and stromal cell migration can be evaluated using image analysis software.

Video Link

The video component of this article can be found at <https://www.jove.com/video/50088/>

Introduction

Solid tumors are comprised of two major compartments: cancer cells and the stromal constituents (both cellular and non-cellular) that assist in maintaining an appropriate environment for tumor growth¹. These stromal constituents play critical roles in the development, progression, and metastasis of many types of cancers, including those of the breast²⁻⁵. The stromal milieu also influences therapeutic responses^{2,4,5}. Thus, determining how cancer cells respond to conventional and novel therapies within the context of the intact microenvironment is important for furthering our understanding of cancer biology and improving current therapeutic strategies. Furthermore, defining how cancer cell-stroma interactions change following the administration of therapy is critical for understanding the biology of tumor relapse.

Organotypic co-culturing systems have been useful for studying tumor-stroma interactions⁶, but it is evident that the methods currently available cannot successfully recapitulate the intact tumor microenvironment *in vitro*, in particular with respect to vascular function and recruitment of immune cells. Indeed, cancer cell responses to therapies that are observed *in vitro* are often significantly different from those observed *in vivo*, where the microenvironment is intact⁵. Thus, *in vivo* models for studying tumor-stroma interactions and their impact on therapeutic response may better reflect clinically relevant mechanisms⁷.

The primary means of studying responses to anti-cancer therapy *in vivo* have been through measurements of tumor size and histological evaluation of tissues derived from treated animals or patients. However, advancements in microscopy and fluorescent reporters over the past two decades have enabled the visualization of inter- and intracellular processes at high resolution in live, anesthetized animals (intravital imaging)⁸. These intravital microscopy technologies have proven to be especially valuable for spatially and temporally dissecting the *in vivo* dynamics of tumor-stroma interactions at cellular and sub-cellular resolution^{8,9}.

Processes that have been unraveled by intravital imaging include anti-tumor T cell cytotoxicity^{10,11}, interactions between T cells and myeloid cells¹², the dynamics of changes in collagen composition and organization following therapeutic treatment¹³, macrophage-dependent cancer cell intravasation and metastasis¹⁴, and vascular permeability¹⁵.

There are three major requirements for intravital imaging. These include appropriate preparation and exposure of tissues for imaging, fluorescent labeling of the tissue components of interest, and a paired microscopy-camera system capable of acquiring images¹⁶. The most common

strategies used to address these requirements include: 1) heterotopic preparations (e.g., inoculation of the ear or eye orbital), permanent imaging windows, or exteriorized preparations (e.g., dorsal skin flap); 2) transgenic fluorescent reporters and fluorescent injectables to label tissue components; and 3) multiphoton or confocal microscopy systems paired with photomultiplier tubes or charge-coupled device (CCD) cameras, respectively⁹. We use a surgically prepared skin flap model to expose the inguinal mammary gland for imaging in anesthetized animals that express transgenes encoding fluorescent reporters. Images are obtained over a period of 12 to 40 hours using an intensified CCD (ICCD) camera paired with a four-laser spinning disk confocal microscope system¹⁷. Imaging in this manner has allowed us to study such processes as *in vivo* drug distribution, stage-dependent chemotherapeutic responses, type of chemotherapy-induced cell death, and myeloid cell behavior⁵.

We provide a protocol for the intravital imaging of cancer cell responses to anti-cancer therapy and tumor-stroma interactions in mouse models of breast cancer. This protocol can be used to track the behaviors and death of both cancer cells and stromal components with a wide variety of transgenic and injectable fluorescent labels in both transgenic and transplantation models for periods of up to 40 hours in a single imaging session.

Protocol

All procedures described must be performed in accordance with guidelines and regulations for the use of vertebrate animals, including prior approval by the local Institutional Animal Care and Use Committee.

1. Generating Mouse Mammary Tumors for Imaging (Transgenic or Orthotopic)

1. Generate mammary tumors for imaging using genetically engineered mouse models (e.g. mouse mammary tumor virus long terminal repeat [MMTV]-polyoma middle T antigen [PyMT] or the rat C3(1) promoter driven large T antigen (Tag) of SV40 [C3(1)-Tag] models) or orthotopic transplantation models (syngeneic, allogeneic, or xenogeneic).
2. Label cancer cells by crossing genetically engineered models with transgenic reporter lines (e.g. ACTB-EGFP) or use *ex vivo* manipulation of primary cancer cells or cell lines (e.g. transduction) followed by transplantation. For a sample protocol for orthotopic transplantation, see¹⁸.

2. Visualizing Components of the Tumor Microenvironment or Sub-cellular Components

1. Visualizing tumor components using transgenic labels. Crossbreed genetically engineered tumor models with transgenic reporter mice (e.g. c-fms-EGFP for myeloid cells or ACTB-H2B-EGFP for nuclei) or use such mice as recipients of transplanted, labeled tissues. This enables visualization of cancer cell-stromal cell interactions in response to therapy or nuclear changes associated with cell death, respectively.
2. Visualizing the microenvironment using injectables. A wide variety of agents (e.g. fluorescently labeled antibodies or chemical dyes) can be used to label various components of the tumor. Depending on the half-life of the dye and the response one is interested in tracking, the injectable may be administered prior to the start of imaging or during the imaging session either intravenously (*i.v.*) or intraperitoneally (*i.p.*, **Figure 1**).

3. Microscopes and Imaging Software

1. Microscope. A variety of microscope systems and software can be used for the imaging of live mice. The most commonly used systems are confocal or multiphoton microscopes. We use a micro-lensed spinning disk confocal microscope (Solamere Technologies, Salt Lake City, UT) with an ICCD camera (XR-Mega-10EX S-30, Stanford Photonics, Palo Alto, CA).
2. Imaging software. We use the open source software μ Manager (Vale Lab, University of California, San Francisco [UCSF]).
3. Image analysis. We use Imaris (Bitplane), Volocity (PerkinElmer), and ImageJ (National Institute of Health [NIH]) for image analysis.

4. (Pre)-treatment of Animals for Imaging

1. Inguinal mammary tumors are optimal for imaging using our protocol when the longest diameter measures approximately 8 mm or less by caliper measurement.
2. For imaging animals treated with a small molecule inhibitor, therapeutic antibody or chemotherapeutic drug, begin treatment prior to or during imaging as required for the experiment. For example, imaging of drug extravasation and distribution requires administration after imaging has been initiated (Movies 1 and 2), while imaging of cell death induced by the chemotherapeutic drug doxorubicin is best captured by starting imaging 24 hr or later after drug treatment (Movies 3 and 4).

5. Preparation of Saline for Maintaining Hydration and Blood Osmolarity of the Animal during Imaging

1. Draw approximately 1 ml of 1x PBS into a 1 ml syringe. Propidium iodide (PI, Invitrogen, 1 mg/ml, diluted 1:15) can be added to this solution that will be periodically administered (*i.p.*) during the imaging session. This will allow for imaging of the nuclei of dead or dying cells that have permeable cell membranes. PI has a very short half-life in the vasculature and must therefore be re-administered throughout the imaging session.
2. Attach a winged infusion set (23 gauge, 3/4 inch needle, 12 inch tubing) to this syringe and push the solution through the tubing until a drop of saline solution exits the tip of the needle at the end of the tubing.
3. Remove the syringe from the infusion set, and refill it with the appropriate saline solution.
4. Re-attach the syringe to the infusion set, taking care not to introduce bubbles into the line.

6. Preparation of the Isoflurane Anesthesia System

1. Add water to the nebulizer and screw it in place. This will humidify the gases delivered to the animal, preventing irritation of the lungs and prolong survival of animals under long-term anesthesia.
2. Fill the isoflurane tank to the top line. CAUTION: Isoflurane is a potent anesthetic that can also affect the researcher. Appropriate vacuum systems should be in place to ensure that excess gases are removed from the area.
3. Turn on both the oxygen tank and the nitrogen tanks and adjust flow. The nitrogen should be at around 1.0 L/min, while the oxygen should be at around 0.2 L/min (~21%).
4. Turn on the (in-house) vacuum. The vacuum should be about 1.2 L/min.
5. Confirm that the anesthesia line to the induction chamber is open, and the lines to the surgery area and the microscope are closed.
6. Confirm that the latex breathing bag attached to the anesthesia system is inflated. If the bag does not inflate, replace it.
7. Check the rubber diaphragm on each of the nose cones delivering anesthesia to the microscope stage and the surgical platform. If the rubber is starting to thin, replace it.

7. Preparation of Surgical Tools and Surgical Platform

1. Turn on a hot bead sterilizer and let it reach >200 °C.
2. Wash the surgical tools in soap and water (one pair of forceps [preferably with teeth] and scissors for cutting through the skin of the animal, one pair of forceps [preferably serrated] and scissors for further exposure of the tumor).
3. Sterilize the surgical tools for at least 30 sec using the hot bead sterilizer (alternatively, the surgical tools can be autoclaved in advance).
4. Let the surgical tools cool off while making sure to avoid contaminating the sterilized tools.
5. Collect the lid to a Styrofoam shipping cooler. This will be your surgical platform.
6. Place a piece of a lab soaker on top of the Styrofoam lid (enough to cover it).
7. Affix a nose cone with a line to the anesthesia system to the lab soaker with laboratory tape (1" tape works best here). Insert an 18 G x1½" needle through the tape into the Styrofoam lid on either side of the nose cone to keep the nose cone secured in place.
8. Set aside betadine, sterile gauze, two 70% isopropanol wipes, a microscope slide, Crazy Glue, and 4 pieces of lab tape (½" width).

8. Preparation of Microscope

1. Turn on the microscope, the camera, and the computer running the microscope.
2. Turn on the heating blanket.
3. If an inverted microscope is to be used, a custom-made stage insert should be designed with imaging ports corresponding to the location of the inguinal mammary glands. Clean the stage insert well with soap and water and dry. Use lab tape (½" works best) to secure cover glass (#1.5 thickness) over the imaging ports and clean the entire surface with 70% isopropanol. Cover the stage with sterile gauze to protect against contamination. Place the stage insert in the stage and allow it to air dry.
4. Tear 4 to 6 pieces of lab tape (1" width), approximately 6 inches in length and attach them to the side of the microscope. These pieces of tape will be used to position the nose cone delivering anesthesia to the animal and fasten it in place.
5. Tear two more pieces of tape (½ inch width) that are about an inch in length. These will be used to keep the butterfly needle delivering PBS to the mouse and the microscope slide used to expose the tumor in place.

9. Exposing the Inguinal Mammary Gland for Imaging

1. Anesthetize the animal in an induction chamber using 4% isoflurane with 21% oxygen and balance nitrogen (flow rate at about 1.0 L/min) as the carrier gas. This should take 2-4 min.
2. Transfer the mouse to the surgical platform once it is breathing deeply and slowly, with the ventral surface facing up. Open the anesthesia line to the surgical platform and then close the anesthesia line to the induction chamber, in this order to avoid too high pressure in the anesthesia system. Reduce the concentration of isoflurane from 4% to 2.5% at this time.
3. Check the pedal withdrawal reflex to confirm that the animal is sufficiently anesthetized for the surgical procedure by performing a footpad pinch. The animal is adequately anesthetized if it does not react (e.g. twitch or curl its tail) to the footpad pinch. If the animal does react to the footpad pinch, increase the concentration of isoflurane.
4. Secure the limbs of the mouse to the surgical platform with laboratory tape (½" tape works best for this).
5. (Optional) Once the animal is secured to the surgical platform, hair can be removed from the ventral surface using an electronic shaver. If chemical hair removal is preferred, this should be performed 24-48 hr prior to surgery. Removing hair prior to surgery helps to prevent contamination of the imaging site, as stray hairs can induce strong and acute immune responses.
6. Disinfect the ventral surface of the animal with 70% isopropanol wipes and betadine.
7. Using the first pair of sterile scissors and forceps (with teeth), make a subcutaneous ventral midline incision that runs from ~3 mm above the urethra to the xiphoid process. Take care to avoid puncturing or cutting through the peritoneum.
8. Using the second pair of sterile scissors and forceps (serrated), gently detach the skin, with the inguinal mammary gland attached, from the peritoneal cavity.
9. Take a glass microscope slide and position it against the skin flap generated in the previous step. Position the slide in such a way that the bulk of the tumor will sit flat once the mouse is placed on the stage, and it does not interfere with the mobility of the hind limbs.
10. Once the microscope slide has been properly positioned, attach the slide to the external surface of the skin using superglue (e.g., Crazy Glue).

10. Positioning the Mouse on the Stage

1. Remove the laboratory tape securing the limbs of the animal to the surgical platform.
2. Open the anesthesia line to the microscope stage and close the anesthesia line to the surgical platform, in this order.
3. Quickly transfer the animal to the microscope stage.
4. Once the animal has been transferred, position and secure the anesthesia line and nose cone properly (using e.g. lab tape) to ensure that the mouse remains anesthetized and is in a comfortable position.
5. Expose the tumor so that it is positioned on top and in the center of one of the cover glass-covered imaging ports in the microscope stage.
6. Using the eyepieces, verify that the tumor is correctly positioned, and gently tape down the microscope slide. The slide should be secured loosely so blood flow to the tissue is not obstructed. Taping down the microscope slide helps to minimize imaging artifacts introduced by the animal's breathing.
7. Insert the indwelling intraperitoneal line with winged infusion set attached to a 1-ml syringe containing sterile 1x PBS or saline (optionally containing a dye such as PI) prepared under #5. Inject the animal with 100 μ l when the *i.p.* line is inserted. From this time point until the end of the imaging session, inject the animal with 50 μ l of saline at 1 hr intervals (or 25 μ l of saline with PI every 30 min).
8. To monitor the animal's vital signs, attach an oximeter probe (e.g. MouseOx system by Starr Life Sciences, Inc.)¹⁹.
9. Cover the mouse with a heating blanket to prevent hypothermia.

11. Acquisition of Images

The open source software μ Manager (Vale Lab, UCSF) is used to acquire time-lapse images. The raw data is compiled in Imaris (Bitplane) software, and can be scored manually by independent observers, or analyzed in either Imaris or other image analysis software (e.g. Volocity [PerkinElmer] or ImageJ [NIH]).

12. Euthanasia

At the end of the image session (1-40 hr, depending on the type of process analyzed), the animal is euthanized.

1. The concentration of isoflurane is increased to 4%.
2. The animal is observed until 30 sec after it ceases breathing and then removed from the stage.
3. Cervical dislocation is performed to ensure that the animal has been euthanized.

13. Representative Results

Intravital imaging using this method allows for the direct visualization of various processes, including drug delivery to tumors, extravasation and distribution of the drug once it reaches the tumor, cell death following therapeutic treatment, and tumor-stroma interactions in response to cell death⁵. To observe the arrival of a drug to the tumor and its distribution following extravasation into tumor tissues, the animal is injected while images are being acquired. Although several classes of chemotherapeutics are weakly fluorescent (such as doxorubicin), many are not. Fluorescently conjugated dextrans can be used as surrogate markers for drug delivery and diffusion into tissues. **Figure 2** and **Movie 1** show the arrival of a fluorescein-isothiocyanate (FITC)-conjugated 2 MD dextran (Invitrogen, 1 mg/ml 1xPBS) injected *i.v.* into a tumor of an MMTV-PyMT;ACTB-ECFP mouse.

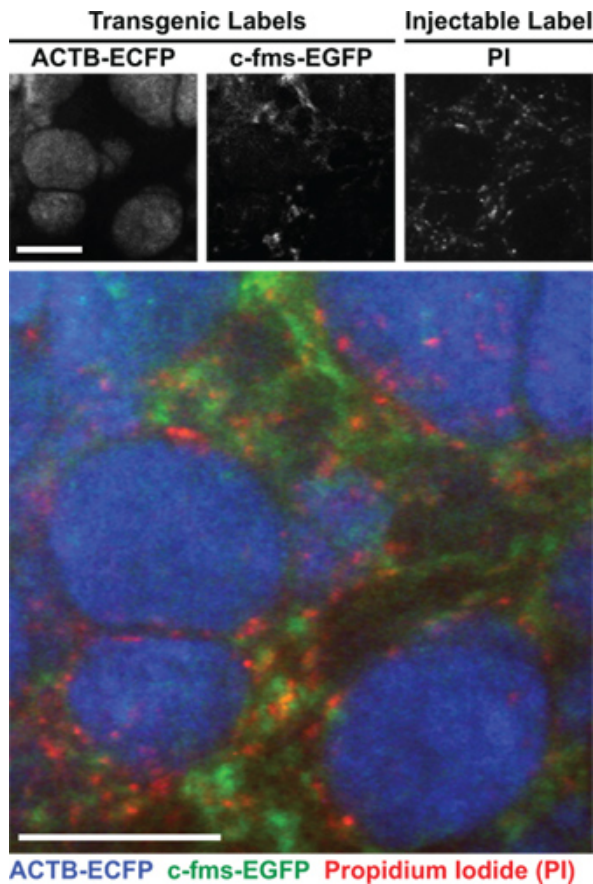
Following the arrival of the drug into the tumor, extravasation and diffusion through the tissues can be imaged to determine both the intravascular half-life of a drug and drug distribution⁵. **Movie 2** shows the extravasation and distribution of Alexa Fluor-647-conjugated 10 kD dextran (Invitrogen, 1 mg/ml in 1 x PBS) injected *i.v.* into a C3(1)-Tag;ACTB-ECFP;c-fms-EGFP mouse during imaging. After compilation of time-lapse movies in Imaris (Bitplane), intravascular half-life and drug distribution is quantified. To measure intravascular half-life, the mean fluorescence intensity in tumor blood vessels at each time point is calculated and plotted against time. Drug distribution is quantified as a percent area per total tumor area that is positive for the drug.

In addition to tracking the kinetics of drug delivery to tumors, it is frequently important to determine how tumors are responding to therapy. As anti-cancer therapies are expected to induce cell death, propidium iodide (PI) staining or structural nuclear changes can be used as a marker of drug-induced cell death⁵. **Figure 3** shows the tumor response to the cytotoxic chemotherapeutic doxorubicin in an MMTV-PyMT;ACTB-ECFP;c-fms-EGFP mouse. In this triple transgenic MMTV-PyMT;ACTB-ECFP;c-fms-EGFP animal, ECFP labels breast cancer cells (blue), and EGFP labels myeloid cells (green). The animal imaged during this session was administered doxorubicin 18 hr before imaging began and PI was delivered *i.p.* throughout the imaging session as described above. Cancer cells (ACTB-ECFP labeling) appear as blue, and dead or dying cells appear as red (PI staining). The time series presented here shows induction of doxorubicin-dependent cell death over time. To quantify the induction of cell death in tumors, the same type of analysis used for determining drug distribution is used, where the quantitative output is percent area per total tumor area that is positive for PI.

Imaging at high magnification can provide information regarding the type of cell death that cancer cells undergo⁵. **Movie 3** shows the results of an imaging experiment to track nuclear changes typical of apoptotic cell death in response to systemic therapy with doxorubicin. To visualize nuclei, the animal imaged during this session harbors the ACTB-H2B-EGFP reporter instead of the c-fms-EGFP reporter, so the nuclei of cancer cells are labeled in green. This MMTV-PyMT;ACTB-ECFP;ACTB-H2B-EGFP animal was administered doxorubicin (8 mg/kg in 1 x PBS) *i.p.* 24 hr prior to the start of movie, and received hourly injections of 1 x PBS containing PI (Invitrogen, 1 mg/ml solution diluted 1:15). Structural changes in the nuclei of cancer cells can be observed in an apoptotic cell next to cells that have undergone necrosis (PI-positive cells that display minimal changes in nuclear morphology). Nuclei of apoptotic cells eventually becomes red due to the uptake of PI staining (not shown). The number of necrotic and apoptotic events is quantified manually for each time point based on PI-positivity and nuclear morphology.

Chemotherapy-induced cancer cell death frequently results in a reactive recruitment of immune cells into tumors^{2,4,5}. **Figure 4** shows an example of this stromal response to acute treatment with doxorubicin. The MMTV-PyMT;ACTB-ECFP;c-fms-EGFP animal imaged here was administered doxorubicin (8 mg/kg in 1 x PBS) *i.p.* approximately 20 hours prior to the start of imaging, and received hourly PI injections *i.p.* for the duration of the experiment to visualize cell death. The times indicated represent the number of hours after doxorubicin treatment, and the scale bar represents 100 μ m. In this experiment, myeloid cells infiltrate into areas of cell death, as indicated by the white arrows. To quantify myeloid cell infiltration into tumors following doxorubicin administration, the same type of analysis used for determining drug distribution and tumor response to chemotherapy is used, where the quantitative output is percent area per total tumor area that is positive for EGFP.

In addition to visualizing the overall stromal response to chemotherapy, specialized stromal responses can also be visualized⁵. Movie 4 shows the phagocytosis of necrotic cell material by a neighboring cell. The red nuclear material can be seen being ingested by a cell with a large intact green nucleus, which is typical of macrophages. The MMTV-PyMT;ACTB-ECFP;ACTB-H2B-EGFP animal imaged during this session was administered doxorubicin (8 mg/kg in 1 x PBS) *i.p.* 24 hr prior to the start of the movie. The animal received hourly injections of 1 x PBS containing PI (Invitrogen, 1 mg/ml solution diluted 1:15). Nuclei (ACTB-EGFP labeling) appear as green, but turn red as the cell undergo necrosis.



ACTB-ECFP c-fms-EGFP Propidium iodide (PI)
Figure 1. Sample labeling of different tumor components using transgenic and injectable labels. This is a triple-transgenic MMTV-PyMT;ACTB-ECFP;c-fms-EGFP animal in which cancer cells are labeled in blue through expression of ECFP and myeloid cells are labeled in green through expression of EGFP from a myeloid-specific promoter. The animal was injected with propidium iodide (PI, red, ~0.07 mg/ml in 1x PBS) during the imaging session to visualize cell death. PI labels DNA but only crosses the cell membranes of dead or dying cells. Scale bar = 100 μ m.

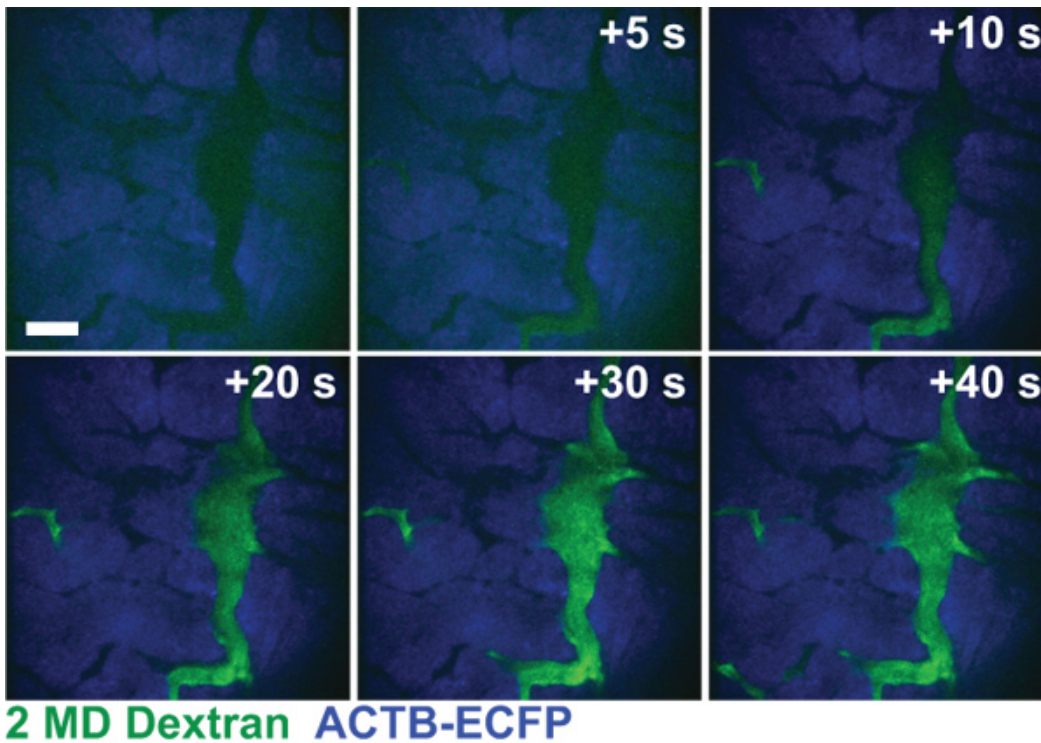


Figure 2. Drug extravasation and distribution in tumors. This double-transgenic MMTV-PyMT;ACTB-ECFP animal in which cancer cells are labeled in blue through expression of ECFP was injected with FITC-conjugated 2 MD dextran (green) during the imaging session to visualize how drugs reach tumors after *i.v.* injection (blue). Time after imaging was initiated is indicated. Scale bar = 100 μ m.

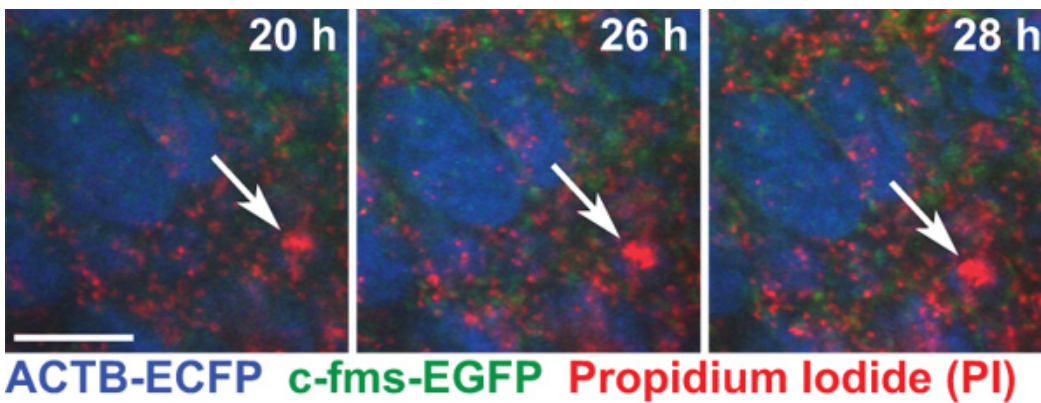
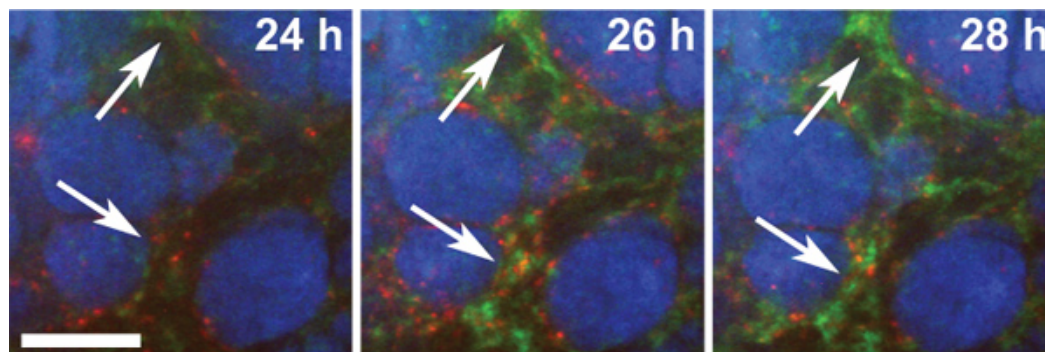


Figure 3. Cancer cell response to systemic therapy. An MMTV-PyMT;ACTB-ECFP;c-fms-EGFP animal treated with the chemotherapeutic drug doxorubicin prior to imaging, and injected with PI (red, ~0.07 mg/ml in 1x PBS) to label cell death. This image series shows the accumulation of PI staining over time (as indicated by white arrows), representing the induction of cell death following doxorubicin treatment. Time indicated is time after doxorubicin treatment. Images are maximum intensity projections of a z-stack containing three images in the z-axis. Scale bar = 100 μ m.



ACTB-ECFP c-fms-EGFP Propidium Iodide (PI)

Figure 4. Myeloid cell response to chemotherapy in an MMTV-PyMT;ACTB-ECFP;c-fms-EGFP triple transgenic mouse administered doxorubicin 20 hr prior to imaging. The animal received hourly *i.p.* injections of PI (red, ~0.07 mg/ml in 1x PBS) to label dead cells. This image series shows the accumulation of EGFP-positive myeloid cells (as indicated by white arrows) over time following doxorubicin treatment. This reactive immune response has been shown to impede therapeutic response to several classes of chemotherapies^{4,5}. Time indicated is time after doxorubicin treatment. Images are maximum intensity projections of a z-stack containing three images in the z-axis. Scale bar = 100 μ m.

Movie 1. Drug delivery into a tumor. This is a double-transgenic MMTV-PyMT;ACTB-ECFP animal in which cancer cells are labeled in blue through expression of ECFP. The animal was injected with a 2 MD FITC-conjugated dextran (green) during the imaging session to visualize how drugs reach tumors after *i.v.* injection. Scale bar = 100 μ m. [Click here to view movie.](#)

Movie 2. Drug infiltration into the tumor tissue. A triple transgenic C3(1)-Tag;ACTB-ECFP;c-fms-EGFP animal in which cancer cells are labeled in blue through expression of ECFP and myeloid cells labeled in green through expression of EGFP was injected *i.v.* with an Alexa Fluor 647-conjugated 10 kD dextran (red). The field of view is shown immediately after injection with dextran. The dextran initially labels the vasculature, rapidly extravasates into the tumor tissue, and is finally taken up by macrophages. Scale bar = 100 μ m. [Click here to view movie.](#)

Movie 3. Imaging of nuclear changes after chemotherapy-induced cell death. This triple transgenic MMTV-PyMT;ACTB-ECFP;H2B-EGFP animal was injected with doxorubicin prior to imaging. Nuclear morphology (green), as tracked by expression of an H2B-EGFP fusion protein, allows for direct visualization of chemotherapy-induced nuclear structural changes typical of apoptosis as seen for the cell in the top right corner. The animal received half-hourly *i.p.* injections of PI (red) for the duration of the imaging session to label dead and dying cells. Time indicated is time after doxorubicin treatment +24 hr. Images were acquired using a high magnification objective lens (40x, NA 1.1, water lens). Scale bar = 15 μ m. [Click here to view movie.](#)

Movie 4. Imaging of nuclear changes and uptake of dead cell material after chemotherapy-induced cell death. This triple transgenic MMTV-PyMT;ACTB-ECFP;H2B-EGFP animal was injected with doxorubicin prior to imaging. Nuclear morphology (green), as tracked by expression of an H2B-EGFP fusion protein, allows for direct visualization of chemotherapy-induced nuclear structural changes. The animal received half-hourly *i.p.* injections of PI (red) for the duration of the imaging session to label dead and dying cells. Images were acquired using a high magnification objective lens (40 x, NA 1.1, water lens). The lack of major structural changes prior to labeling with PI and the change in the nuclear morphology and loss of GFP signal is indicative of necrosis-like cell death. The dead material is seen being taken up by a cell with a large nucleus, which is typical of macrophages. Time indicated is time after doxorubicin treatment +24 hr. Scale bar = 10 μ m. [Click here to view movie.](#)

Discussion

The responses of tumors to systemic therapies *in vivo* can be dramatically different to those of cancer cells *in vitro*, as the microenvironment influences both the acute response and relapse⁵. One of the biggest obstacles to explicating *in vivo* chemoresistance pathways is the complexity of the interactions between cancer cells and their microenvironment. In particular, because solid tumors have developed a balance between cancer and stromal cells, perturbations of one component, such as the cell death that occurs during anti-cancer treatment, can result in dramatic effects on tissue organization.

The intravital imaging technique provided here allows for the direct visualization of cancer cell-stroma interactions within the tumors of live, anesthetized mice during treatment with anti-cancer drugs. We use spinning disk confocal microscopy, which has a relative limited penetration depth (see¹⁷), but our surgical and labeling techniques can be used with other types of microscopy. Movies acquired from these experiments can be used to track processes that include changes in fluorescence intensity (e.g. due to infiltration of a labeled population or induction of cell death), cell motility, distribution of injectables (e.g. to track vascular leakage), and co-localization of fluorescent signals^{5,12,17,20}.

We routinely image mice for over 6 hours and also performed imaging for over 18 hours. This requires maintaining the mice continuously under anesthesia for these long time periods. With proper anesthesia, over 90% of our animals survive 6 hours, and about 80% survive over 18 hours. Details on how to perform long-term anesthesia have been published previously¹⁹. In our experience, five factors are critical: avoiding hypothermia, avoiding dehydration, maintaining physiological blood oxygen saturation levels, using humidified carrier gas for isoflurane, and keeping the animals at the lowest level of anesthesia at which they do not show signs of pain. To maintain body temperature, we keep mice under a heated blanket (at 38 °C). To avoid dehydration, we inject small volumes of saline *i.p.* throughout the entire imaging procedure. To maintain physiological blood oxygen saturation levels, we start with 21% oxygen in the carrier gas (rather than the commonly used 100%). This enables us to increase inhaled oxygen levels if a mouse - hours into an experiment - shows a decrease in blood oxygen saturation. In our experience, increasing the inhaled oxygen levels at such time (e.g. to 30-40%) almost always will stabilize the animal allowing for hours of additional imaging. The optimal level of anesthesia is for most mice achieved with 1-1.5% isoflurane and results in breath rates of 60-65/min

and pulse rates of 400-450/min. In our imaging experiments, we primarily use transgenic mouse models (MMTV-PyMT and C3[1]-Tag) in which tumors are multifocal, allowing for imaging of multiple lesions at different stages of tumor progression in parallel at multiple x,y positions during a single imaging session. This decreases concerns regarding mouse-to-mouse variation with respect to experiments aimed at identifying stage-dependent therapeutic responses, and reduces the number of animals required for imaging.

The MMTV-PyMT model (and other spontaneous cancer models) go through progressive histopathological stages that can be recognized during intravital imaging, although the pathological staging of tumor lesions that can be done during intravital imaging is different from, and less detailed, than that of histological sections^{5,17}. In contrast, transplantation models tend to reflect late stage tumors best, as the cancer cells usually are isolated from advanced tumors. Such models are thus more amenable to studying tumor-stroma interactions of late stage tumors than differences in these interactions between different stages.

We show examples of how to image nuclear structural changes that occur after cell death induced by therapy. In the absence of anti-cancer treatment, this labeling strategy may instead be used to image cell division *in situ*, elucidating, for example, how cell proliferation and dormancy is influenced by the microenvironment. In the future, fluorescent labeling of mitochondrial components may make it possible to image mitochondrial changes that occur during apoptotic cell death.

In this protocol, we have also shown examples of how to image cancer cell-immune cell interactions after therapy, but other microenvironmental components can also be visualized and imaged. Existing transgenic reporter lines for stromal components include those for fibroblasts (e.g., FSP1-EGFP¹⁷, α SMA-RFP²¹, COL1A1-EGFP²¹) or cells of the vasculature (e.g. Tie2-GFP²², VEGF-GFP²³).

Intravital imaging allows for the real-time visualization of the interactions and processes that occur *in vivo* following chemotherapy administration. With the technology currently available, we have made major progress in understanding how myeloid cells influence therapeutic response; however, because the tumor microenvironment is so complex, major advancements are still needed to begin to delve mechanistically into the processes underlying environment-mediated drug resistance. One of the most important advancements still required is the identification of better markers for specific cell populations. The importance of better markers is well illustrated with two of the most prominent stromal cell components of the breast tumor microenvironment, fibroblasts and immune cells. α -Smooth muscle actin (α SMA) is frequently used to identify fibroblasts, but the protein is also expressed by vascular smooth muscle cells and myoepithelial cells²⁴. Thus, although α SMA-GFP reporter mice exist, determining the specific cell type being followed during an intravital imaging experiment is challenging. Similarly, a single fluorescent marker such as EGFP expressed under the c-fms promoter will often identify multiple subpopulations of immune cells^{12,17}. Thus, although one would ideally like to use a single marker to identify a specific cell type the complexity of the underlying biology poses a major challenge in using this approach.

One partial solution to this problem is to use injectable labels to further differentiate subpopulations of cells expressing the same fluorescent reporter. For example, fluorescent dextrans are taken up by macrophages and can be used to label the macrophage subpopulations that are labeled by the c-fms-EGFP and Fsp1-EGFP transgenic reporter mice¹⁷. Antibodies conjugated to fluorescent probes have also been used to identify specific subpopulations (e.g. the Gr1-positive population of myeloid cells labeled by the c-fms-EGFP reporter¹⁷).

Unlike tumor response curves generated by caliper measurement, which provide little mechanistic information about how or why tumors respond to the administered therapeutic, or histological series derived from tissues harvested at different time points that require large cohorts of animals, our technique provides direct, quantifiable information on the dynamics of cell death and on the interactions of stromal cells with cancer cells in small cohorts. Thus, the advantage of using the procedure reported here is that it provides dynamic information on drug responses in the context of an intact tumor microenvironment in real-time. Such information can lead to important insights into the underlying processes that drive therapeutic responses⁵.

Disclosures

The authors have no conflicts of interest to disclose. All animal experiments were conducted in accordance with IACUC approved protocols.

Acknowledgements

We thank J. Cappellani and J. Qiu for technical support. This work was supported by funds from the National Cancer Institute (U01 CA141451), the Starr Cancer Consortium, Susan G. Komen for the Cure, Long Island 2 Day Walk to Fight Breast Cancer, Manhasset Women's Coalition Against Breast Cancer to M.E., and a pre-doctoral fellowship from the Congressionally Directed Breast Cancer Research Program, U.S. to E.S.N. E.S.N. is also the recipient of the Leslie C. Quick and William Randolph Hearst Foundation Fellowships from the Watson School of Biological Sciences. H.A.A. was supported by funds from the Research Council of Norway (160698/V40 and 151882), and Southeastern Regional Health Authorities (2007060).

References

1. Egeblad, M., Nakasone, E.S., & Werb, Z. Tumors as organs: complex tissues that interface with the entire organism. *Dev. Cell* **18**, 884-901, doi: 10.1016/j.devcel.2010.05.012 (2010).
2. Ahn, G-O., Tseng, D., Liao, C.-H., Dorie, M.J., Czechowicz, A., & Brown, J.M. Inhibition of Mac-1 (CD11b/CD18) enhances tumor response to radiation by reducing myeloid cell recruitment. *Proc. Natl. Acad. Sci. U.S.A.* **107**, 8363-8368, doi:10.1073/pnas.0911378107 (2010).
3. Tlsty, T.D. & Coussens, L.M. Tumor stroma and regulation of cancer development. *Annu. Rev. Pathol.* **1**, 119-150, doi:10.1146/annurev.pathol.1.110304.100224 (2006).
4. DeNardo, D.G., Brennan, D.J., *et al.* Leukocyte complexity predicts breast cancer survival and functionally regulates response to chemotherapy. *Cancer Discov.* **1**, 54-67, doi:10.1158/2159-8274.CD-10-0028 (2011).

5. Nakasone, E.S., Askautrud, H.A., *et al.* Imaging tumor-stroma interactions during chemotherapy reveals contributions of the microenvironment to resistance. *Cancer Cell*. **21**, 488-503 (2012).
6. Kim, J.B., Stein, R., & O'Hare, M.J. Three-dimensional *in vitro* tissue culture models of breast cancer-- a review. *Breast Cancer Res. Treat.* **85**, 281-291, doi: 10.1023/B:BREA.0000025418.88785.2b (2004).
7. Gilbert, L.A. & Hemann, M.T. DNA damage-mediated induction of a chemoresistant niche. *Cell*. **143**, 355-366, doi:10.1016/j.cell.2010.09.043 (2010).
8. Pittet, M.J. & Weissleder, R. Intravital imaging. *Cell*. **147**, 983-991, doi:10.1016/j.cell.2011.11.004 (2011).
9. Lohela, M. & Werb, Z. Intravital imaging of stromal cell dynamics in tumors. *Curr. Opin. Genet. Dev.* **20**, 72-78, doi:10.1016/j.gde.2009.10.011 (2010).
10. Boissonnas, A., Fetler, L., Zeelenberg, I.S., Hugues, S., & Amigorena, S. *In vivo* imaging of cytotoxic T cell infiltration and elimination of a solid tumor. *J. Exp. Med.* **204**, 345-356, doi:10.1084/jem.20061890 (2007).
11. Breart, B., Lemaître, F., Celli, S., & Bousso, P. Two-photon imaging of intratumoral CD8+ T cell cytotoxic activity during adoptive T cell therapy in mice. *J. Clin. Invest.* **118**, 1390-1397, doi: 10.1172/JCI34388 (2008).
12. Engelhardt, J.J. & Boldajipour, B. Marginating dendritic cells of the tumor microenvironment cross-present tumor antigens and stably engage tumor-specific T cells. *Cancer Cell*. **21**, 402-417, doi:10.1016/j.ccr.2012.01.008 (2012).
13. Brown, E., McKee, T., *et al.* Dynamic imaging of collagen and its modulation in tumors *in vivo* using second-harmonic generation. *Nat. Med.* **9**, 796-800, doi: 10.1038/nm879 (2003).
14. Wyckoff, J. B., Wang, Y., *et al.* Direct visualization of macrophage-assisted tumor cell intravasation in mammary tumors. *Cancer Res.* **67**, 2649-2656, doi: 10.1158/0008-5472.CAN-06-1823 (2007).
15. Yuan, F., Salehi, H.A., Boucher, Y., Vasthare, U.S., Tuma, R.F., & Jain, R.K. Vascular permeability and microcirculation of gliomas and mammary carcinomas transplanted in rat and mouse cranial windows. *Cancer Res.* **54**, 4564-4568 (1994).
16. Jain, R.K., Munn, L.L., & Fukumura, D. Dissecting tumour pathophysiology using intravital microscopy. *Nat. Rev. Cancer.* **2**, 266-276, doi:10.1038/nrc778 (2002).
17. Egeblad, M., Ewald, A.J., *et al.* Visualizing stromal cell dynamics in different tumor microenvironments by spinning disk confocal microscopy. *Dis Model Mech.* **1**, 155-67, doi:10.1242/dmm.000596 (2008).
18. Cheng, N. & Lambert, D.L. Mammary Transplantation of Stromal Cells and Carcinoma Cells in C57BL/6J Mice. *J. Vis. Exp.* (54), e2716, doi:10.3791/2716 (2011).
19. Ewald, A.J., Werb, Z., & Egeblad, M. Monitoring of vital signs for long-term survival of mice under anesthesia. *Cold Spring Harb. Protoc.* **2011**, pdb.prot5563, doi:10.1101/pdb.prot5563 (2011).
20. Sounni, N.E., Dehne, K., *et al.* Stromal regulation of vessel stability by MMP14 and TGFbeta. *Dis. Model Mech.* **3**, 317-332, doi:10.1242/dmm.003863 (2010).
21. Magness, S.T., Bataller, R., Yang, L., & Brenner, D.A. A dual reporter gene transgenic mouse demonstrates heterogeneity in hepatic fibrogenic cell populations. *Hepatology*. **40**, 1151-1159, doi:10.1002/hep.20427 (2004).
22. Motoike, T., Loughna, S., *et al.* Universal GFP reporter for the study of vascular development. *Genesis*. **28**, 75-81, doi:10.1002/1526-968X(200010)28:2<75::AID-GENE50>3.0.CO;2-S (2000).
23. Fukumura, D., Xavier, R., *et al.* Tumor induction of VEGF promoter activity in stromal cells. *Cell*. **94**, 715-725, doi:10.1016/S0092-8674(00)81731-6 (1998).
24. Sugimoto, H., Mundel, T.M., Kieran, M.W., & Kalluri, R. Identification of fibroblast heterogeneity in the tumor microenvironment. *Cancer Biol. Ther.* **5**, 1640-1646, doi:10.4161/cbt.5.12.3354 (2006).
25. Ewald, A.J., Werb, Z., & Egeblad, M. Dynamic, long-term *in vivo* imaging of tumor-stroma interactions in mouse models of breast cancer using spinning-disk confocal microscopy. *Cold Spring Harb. Protoc.* **2011**, pdb.top97, doi: 10.1101/pdb.top97 (2011).